

Boundary Control of Traffic Congestion Modeled as a Non-stationary Stochastic Process

Xun Liu and Hossein Rastgoftar

Abstract—In this paper, we introduce a new conservation-based approach to model traffic dynamics, and apply the model predictive control (MPC) approach to manage the boundary traffic inflow and outflow, so that the traffic congestion is reduced. We establish an interface between the Simulation of Urban Mobility (SUMO) software and MATLAB to define a network of interconnected roads (NOIR) as a directed graph, and present traffic congestion management as a network control problem. By formally specifying the traffic feasibility conditions, and using the linear temporal logic, we present the proposed MPC-based boundary control problem as a quadratic programming with linear equality and inequality constraints. The success of the proposed traffic boundary control is demonstrated by simulation of traffic congestion control in Center City Philadelphia.

I. INTRODUCTION

During the urbanization process, numerous negative impacts have been created by the traffic congestion, such as environmental pollution [1], economic recession [2], [3], human physical and mental health harms [4], and ecological destruction [5]. Considering the acceleration of the urbanization process, it is urgent to solve the traffic congestion problem. Some researchers have presented several temporary solutions to reduce traffic congestion, such as building more roads or restricting vehicles; however, these solutions are not in consideration in this paper. We concentrate on finding the optimal solution by constructing and controlling the traffic model.

Over the past years, researchers have proposed a large number of approaches to alleviate traffic congestion. We can divide the approaches into two categories: model-based approaches and model-free approaches. While the model-based approaches rebuild traffic dynamics properties in a traffic model and obtain the optimal solution by applying the appropriate control method to the traffic model, the model-free approaches accomplish the traffic management by replacing the traffic model through an equivalent data model or controlling of the traffic signal plan.

An essential task in the model-based approach is to construct a virtual traffic model to represent the real traffic dynamics' properties. Then, based on this traffic model, appropriate approaches can be applied to control the traffic dynamics or predict the traffic states. The macroscopic fundamental diagram (MFD) of the traffic flow model [6],

which describes the relationship between traffic density and traffic flow, is a widely used approach to describe the traffic dynamics. Ref. [7] verifies the MFD model based on the real traffic data and evaluates the traffic state by applying this model. Moreover, Ref. [8] integrates the perimeter control with the MFD model to improve the traffic network capacity and mobility. To improve the accuracy of the traffic dynamics model, Ref. [9]–[14] integrate the cell transmission model (CTM) approach with the MFD model. Furthermore, the CTM approach, which is widely used to partition the traffic network into road elements, can also incorporate conservation laws to construct the traffic dynamics model [15]–[18]. Moreover, Ref. [19] incorporates the CTM model with the finite-state Markov decision process (MDP) to obtain the optimal movement phases at the traffic junctions. Once the traffic model is generated, the control and optimization methods can be implemented to find the optimal solution. Ref. [8], [16], [19], [20] adopt the model predictive control (MPC) approach to obtain the optimal solution for boundary traffic control and Ref. [17], [21] apply mixed-integer linear programming (MILP) to solve the optimization problem.

Traffic congestion control can also be accomplished through a model-free approach. For example, Ref. [22] uses a data model to represent the traffic dynamics and incorporates adaptive predictive control to adjust the boundary input. Another model-free possibility for reducing congestion is through traffic signal optimization. In recent years, with the rapid development of AI technology and computing capacity, the reinforcement learning (RL) has been increasingly adopted to optimize the traffic signal plan. Ref. [23] proposes a Q-learning algorithm for traffic signal control. Moreover, Ref. [24] integrates the RL with the Markov decision process to reduce computational complexity. Furthermore, Ref. [25] introduces an efficient RL method for traffic signal control in complicated multiple intersections and Ref. [26] summarizes the RL algorithms that have been applied in adaptive traffic signal control (ATSC) in recent years. In addition to the RL approach, a fuzzy controller is also employed by researchers to control the traffic signal [27], [28].

This paper presents further research based on our previous work [15]. In this paper, we continue to use mass conservative law to define the traffic coordination model and describe traffic dynamics. Also, we model the dynamics of the traffic coordinate as a non-stationary stochastic process. Comparing with our previous research, in this paper we modify the definition of the stochastic parameter to improve and perfect the traffic model to make it more realistic. In addition, in the process of determining the optimal boundary

Xun Liu is with the Department of Mechanical Engineering at Villanova University, Villanova, PA 19085, USA xliu8@villanova.edu

Hossein Rastgoftar is with the Department of Aerospace and Mechanical Engineering at the University of Arizona, Tucson, AZ 85721, USA hrastgoftar@arizona.edu



Fig. 1: Example NOIR: Center City, Philadelphia

control solution, we consider and simulate the impact of the current number of road vehicles in the results. Similar to our previous work, the network of interconnected roads (NOIR) is generated by converting the real street map using the software Simulation of Urban Mobility (SUMO) and MATLAB. The road elements in the NOIR are categorized into three groups: "inlet road elements," "outlet road elements," and "interior road elements." We set the boundary traffic flow as the control variable, and accomplish the objective of traffic congestion alleviation by controlling the boundary inflow from the inlet road elements and the boundary outflow from the outlet road elements using the model predictive control (MPC) approach. In the case study, we integrate the proposed traffic model with the MPC approach and illustrate the results of traffic congestion management on the Center City district of Philadelphia (See. Fig. 1).

This paper is organized as follows: Section II gives an introduction about the notions existing in the NOIR and the linear temporal logic symbols used to describe traffic state conditions. The basic principles and definitions for model construction and the traffic feasibility conditions for solving the cost function in boundary control are explained in Section III. The explanation about traffic network dynamics and the traffic control approach are presented in Section IV and Section V, respectively. The simulation results of a case study using the proposed traffic model and control approach in Center City Philadelphia are illustrated in Section VI, followed by the conclusion in Section VII.

II. PRELIMINARIES

A. Graph Theory Notions

The network of inter-connected roads (NOIR) presented in this paper is generated by using the software Simulation of Urban Mobility (SUMO) based on a real street map of Philadelphia. A NOIR can be denoted as a graph $\mathcal{G}(\mathcal{V}, \mathcal{E})$, where set $\mathcal{V} = \{1, \dots, N\}$ defines N road elements and set

$\mathcal{E} \subset \mathcal{V} \times \mathcal{V}$ determines the interconnections between the road elements. As shown in Fig. 1, every element $i \in \mathcal{V}$ is a unidirectional street and located between two consecutive junctions. Element $(i, j) \in \mathcal{E}$ represents the connection directed from road element $i \in \mathcal{V}$ to road element $j \in \mathcal{V}$. Set \mathcal{V} can be divided into three subsets: the inlet road elements set $\mathcal{V}_{in} = \{1, \dots, N_{in}\}$, the outlet road elements set $\mathcal{V}_{out} = \{N_{in} + 1, \dots, N_{out}\}$, and the interior road elements set $\mathcal{V}_I = \{N_{out} + 1, \dots, N\}$. For every road element $i \in \mathcal{V}$, we define in-neighbor set \mathcal{I}_i and out-neighbor set \mathcal{O}_i as follows:

$$\mathcal{I}_i = \{j | (j, i) \in \mathcal{E}\}, \quad (1a)$$

$$\mathcal{O}_i = \{j | (i, j) \in \mathcal{E}\}, \quad (1b)$$

where the in-neighbor and out-neighbor road elements refer to the upstream adjacent road elements and downstream adjacent road elements. Note that the in-neighbor set of every inlet road element and the out-neighbor set of every outlet road element are empty, i.e., $\mathcal{I}_i = \emptyset$, if $i \in \mathcal{V}_{in}$ and $\mathcal{O}_i = \emptyset$, if $i \in \mathcal{V}_{out}$.

B. Linear Temporal Logic

We use the linear temporal logic (LTL) to describe the properties and feasible conditions of the traffic dynamics model. A LTL formula normally consists of three components, the propositional variables, the logical operators, and the temporal modal operators [29]. Propositional variable is the most fundamental element in the propositional logic whose value is either true or false. The logical operators, such as *negation* (\neg), *disjunction* (\wedge) and *conjunction* (\vee), can act on a single propositional variable or between multiple propositional variables to express a sophisticated logical formula accurately. The temporal modal operators including *eventually* (\diamond), *always* (\square), *next* (\circ), and *until* (\mathcal{U}), define the temporal variables of LTL formulas [30].

Inspired by Metric Temporal Logic (MTL) [16], [31], we extend the classic LTL by integrating the temporal modal operators with a distance function to restrict the logical formula into a finite domain. For example, assuming $\mathcal{T} = \{0, \dots, N_{\mathcal{T}} | 0 < N_{\mathcal{T}} < \infty\}$ is a finite time domain, the formula $\square_{\mathcal{T}}(\cdot)$ at sampling time k means that the statement expressed in the parenthesis is always true at every time $k+t$, where $t \in \mathcal{T}$.

III. PROBLEM STATEMENT

In this paper, we consider the traffic dynamics as a physical model which satisfies the mass conservation law and describe the dynamics in every road element $i \in \mathcal{V}$ as follows:

$$\rho_i[k+1] = \rho_i[k] + y_i[k] - z_i[k] + s_i[k] \quad (2)$$

where $k = 1, 2, \dots$ denotes the discrete sampling time, $\rho_i[k]$ is the number of existing cars at road element i , and called *traffic density*. Also, $y_i[k]$, $z_i[k]$ and $s_i[k]$ are the network traffic inflow, network traffic outflow and the external traffic flow, respectively.

The external traffic flow $s_i[k]$, which is defined in Eq. (3), specifies the traffic exchange between the NOIR and the external environment. It is prescribed that, at every sampling interval $[t_k, t_{k+1})$ the traffic could only drive into the NOIR through the inlet road elements, defined by \mathcal{V}_{in} , and depart from the NOIR through the outlet road elements, defined by \mathcal{V}_{out} . Therefore, we define $s_i[k]$ by

$$s_i[k] = \begin{cases} u_i[k] \geq 0 & i \in \mathcal{V}_{in} \\ -v_i[k] \leq 0 & i \in \mathcal{V}_{out} \\ 0 & i \in \mathcal{V}_I \end{cases} \quad (3)$$

at every discrete time k , where $u_i[k] \geq 0$ is the number of cars entering the NOIR through \mathcal{V}_{in} and $v_i[k] \geq 0$ is the number of cars leaving the NOIR through \mathcal{V}_{out} .

The network traffic inflow $y_i[k]$ and traffic outflow $z_i[k]$ given by Eq. (4) determine the traffic flow exchange between road elements within the NOIR at every discrete sampling time k , and defined by

$$y_i[k] = \begin{cases} 0 & i \in \mathcal{V}_{in} \\ v_i[k] & i \in \mathcal{V}_{out}, \\ \sum_{j \in \mathcal{I}_i} q_{i,j}[k] z_j[k] & i \in \mathcal{V}_I \end{cases}, \quad (4a)$$

$$z_i[k] = \begin{cases} u_i[k] & i \in \mathcal{V}_{in} \\ 0 & i \in \mathcal{V}_{out}, \\ p_i[k] (\rho_i[k] + y_i[k]) & i \in \mathcal{V}_I \end{cases}, \quad (4b)$$

where

$$p_i[k] = \begin{cases} 1 & \text{If } i \in \mathcal{V}_{in} \cup \mathcal{V}_{out} \\ 0 & \text{If } i \in \mathcal{V}_I \text{ and } y_i + \rho_i = 0 \\ \frac{z_i[k]}{\rho_i[k] + y_i[k]} & \text{If } i \in \mathcal{V}_I \text{ and } y_i + \rho_i \neq 0 \end{cases} \quad (5)$$

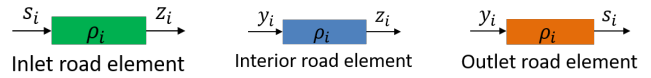
is the fraction of inflow and outflow of road $i \in \mathcal{V}$ that leaves $i \in \mathcal{V}$ during sampling interval $[t_k, t_{k+1})$. Also, $q_{i,j}[k] \in [0, 1]$ in Eq. (4a) is the fraction of cars driving from road element $j \in \mathcal{V} \setminus \mathcal{V}_{out}$ to each of its downstream adjacent road elements $i \in \mathcal{V}$ at every sampling time k . Therefore, $q_{i,j}[k]$ must satisfy the following equality constraint:

$$\sum_{i \in \mathcal{O}_j} q_{i,j} = 1. \quad (6)$$

Note that the flow probability $p_i[k]$ and fraction probability $q_{i,j}[k]$ reflect the uncertainty caused by human driver intentions. Therefore, our proposed model consistently incorporates the human intent into modeling of traffic coordination. In this paper, we assume that the flow probability $p_i[k]$ and fraction probability $q_{i,j}[k]$ are known but they are randomly generated at every road $i \in \mathcal{V}$ and every discrete time $k = 0, 1, 2, \dots$. Fig.2 illustrates the traffic flow at inlet road element, interior road element and outlet road element.

Assumption 1. *In the process of building the traffic dynamics model, we assume that the time increment $\Delta T = t_{k+1} - t_k$ is constant and sufficiently small such that the flow probability $p_i[k]$ satisfies the following condition:*

$$p_i[k] = \begin{cases} \frac{z_i[k]}{\rho_i[k] + y_i[k]} \in [0, 1) & \text{If } \rho_i[k] + y_i[k] \neq 0 \\ 0 & \text{If } \rho_i[k] + y_i[k] = 0 \end{cases}. \quad (7)$$



(a) Inlet road element $i \in \mathcal{V}_{in}$ (b) Interior road element $i \in \mathcal{V}_I$ (c) Outlet road element $i \in \mathcal{V}_{out}$

Fig. 2: Traffic flows in inlet road element, interior road element and outlet road element

In this paper, we offer an MPC-based boundary control to manage the traffic congestion in the NOIR. Therefore, boundary input s_i is determined at every road $i \in \mathcal{V}_{in} \cup \mathcal{V}_{out}$ by solving a quadratic programming problem with the cost function and constraints that are described below:

Traffic Coordination Cost: We define

$$C = \frac{1}{2} \sum_{j=k+1}^{k+N_\tau} \left(\sum_{i \in \mathcal{V}_{in} \cup \mathcal{V}_{out}} s_i^2[j-1] + \beta \sum_{l \in \mathcal{V}_I} \rho_l^2[j] \right) \quad (8)$$

as the traffic coordination cost, where $s_i = u_i$ for every inlet road element $i \in \mathcal{V}_{in}$, $s_i = v_i$ for every outlet road element $i \in \mathcal{V}_{out}$, and $\beta > 0$ is a constant scaling parameter, which reflects the influence weight of the number of existing cars on the interior road element ρ_l on the criterion function C .

State Feasibility Condition: Traffic density is set to be a non-negative physical parameter. Moreover, we assume every road element in the NOIR holds a maximal capacity ρ_{max} and the traffic density of the road element can not exceed this maximal value within the next N_τ time steps at every sampling time k . We define a LTL formula π_1 to express these state constrains at every interior road element $i \in \mathcal{V}_I$ by

$$\pi_1 := \bigwedge_{i \in \mathcal{V}_I} \square_{\mathcal{T}} (\rho_i > 0 \wedge \rho_i < \rho_{max}). \quad (9)$$

Input Feasibility Condition: At every sampling time k , back-flow must be prohibited at every boundary road element $i \in \mathcal{V}_{in} \cup \mathcal{V}_{out}$ within the next N_τ sampling times. We express this feasibility condition using the LTL formula π_2 :

$$\pi_2 := \bigwedge_{i \in \mathcal{V}_{in}} \bigwedge_{j \in \mathcal{V}_{out}} \square_{\mathcal{T}} (u_i \geq 0 \wedge v_j \geq 0) \quad (10)$$

Input Optional Condition: We assume that the demand for entering and leaving the NOIR is high and only d_0 amount of cars are permitted to cross the boundary of the NOIR within the next N_τ sampling times at every discrete time k . Therefore, the following LTL formula must be satisfied:

$$\pi_3 := \square_{\mathcal{T}} \left(\sum_{i \in \mathcal{V}_{in}} u_i + \sum_{j \in \mathcal{V}_{out}} v_j = d_0 \right) \quad (11)$$

IV. TRAFFIC NETWORK DYNAMICS

We substitute Eqs. (3) and (4) into Eq. (2) and simplify the traffic dynamics for every road element $i \in \mathcal{V}$ as follows:

$$\forall i \in \mathcal{V}_{in} \cup \mathcal{V}_{out}, \quad \rho_i[k+1] = \rho_i[k] \quad (12a)$$

$$\forall i \in \mathcal{V}_I, \rho_i[k+1] = (1 - p_i[k]) \left(\rho_i[k] + \sum_{j \in \mathcal{I}_i} q_{i,j}[k] z_j[k] \right). \quad (12b)$$

Eq. (12) implies that the traffic density remains constant at every road $i \in \mathcal{V}_{in}$ but it is updated with time at every interior road elements $i \in \mathcal{V}_I$. As a result, the network traffic dynamics are only defined over the interior road elements. To obtain the traffic dynamics, we define the state vector $\mathbf{x} = [\rho_{N_{out}+1} \ \cdots \ \rho_N]^\top \in \mathbb{R}^{(N-N_{out}) \times 1}$, the inflow vector $\mathbf{y} \in \mathbb{R}^{(N-N_{out}) \times 1}$, and the outflow vector $\mathbf{z} \in \mathbb{R}^{(N-N_{out}) \times 1}$. Moreover, we define the outflow probability matrix $\mathbf{P} \in \mathbb{R}^{(N-N_{out}) \times (N-N_{out})}$ and the tendency probability matrix $\mathbf{Q} \in \mathbb{R}^{(N-N_{out}) \times (N-N_{out})}$ as follows:

$$\mathbf{P}[k] = \text{diag}(p_{N_{out}+1}[k], \dots, p_N[k]), \quad (13a)$$

$$\mathbf{Q}[k] = [Q_{ij}[k]] = [q_{i+N_{out}, j+N_{out}}[k]], \quad (13b)$$

where $Q_{ij} = q_{i+N_{out}, j+N_{out}}$ determines the fraction of departing vehicles driving from road element $(j+N_{out}) \in \mathcal{V}_I$ towards road element $(i+N_{out}) \in \mathcal{V}_I$ at discrete time k .

By considering definitions of traffic inflow and outflow given in Eq. (4), the network inflow vector \mathbf{y} and network outflow vector \mathbf{z} are related to state vector \mathbf{x} by

$$\mathbf{y}[k] = (\mathbf{I} - \mathbf{Q}[k]\mathbf{P}[k])^{-1} \mathbf{Q}[k]\mathbf{P}[k]\mathbf{x}[k], \quad (14a)$$

$$\mathbf{z}[k] = \left(\mathbf{P}[k] (\mathbf{I} - \mathbf{Q}[k]\mathbf{P}[k])^{-1} \mathbf{Q}[k]\mathbf{P}[k] + \mathbf{P}[k] \right) \mathbf{x}[k], \quad (14b)$$

at every sampling time k , and the traffic dynamics can be expressed in the state space form by

$$\mathbf{x}[k+1] = \mathbf{A}[k]\mathbf{x}[k] + \mathbf{B}[k]\mathbf{s}[k]. \quad (15)$$

In Eq. (15), $\mathbf{s}[k] = [s_i[k]] \in \mathbb{R}^{N_{out} \times 1}$, $\mathbf{B}[k] = b_{i,j}[k] \in \mathbb{R}^{(N-N_{out}) \times N_{out}}$, and $\mathbf{A}[k] \in \mathbb{R}^{(N-N_{out}) \times (N-N_{out})}$ refer to the input vector, the input matrix, and the system matrix at every sampling time k , where

$$s_i[k] = \begin{cases} u_i[k], & \text{If } i \in \mathcal{V}_{in} = \{1, \dots, N_{in}\} \\ v_i[k], & \text{If } i \in \mathcal{V}_{out} = \{N_{in}+1, \dots, N_{out}\} \end{cases}, \quad (16a)$$

$$b_{ij}[k] = \begin{cases} 1 & j \in \mathcal{I}_{i+N_{out}} \\ -1 & j \in \mathcal{O}_{i+N_{out}} \end{cases}, \quad (16b)$$

$$\begin{aligned} \mathbf{A}[k] &= (\mathbf{I} - \mathbf{P}[k]) \left(\mathbf{I} + (\mathbf{I} - \mathbf{Q}[k]\mathbf{P}[k])^{-1} \mathbf{Q}[k]\mathbf{P}[k] \right) \\ &= (\mathbf{I} - \mathbf{P}[k]) (\mathbf{I} - \mathbf{Q}[k]\mathbf{P}[k])^{-1}. \end{aligned} \quad (16c)$$

Theorem 1. *The traffic dynamics (15) is bounded-input bounded-output (BIBO) stable, when the following premises are satisfied:*

- 1) Vehicles can only enter the NOIR through an inlet road element and exit from the NOIR through an outlet road element.
- 2) The out-neighbors of an inlet road element are all interior road elements, i.e. if $i \in \mathcal{V}_{in}$, then, $\mathcal{O}_i \subset \mathcal{V}_I$.
- 3) Vehicles entering the NOIR through an inlet road element departs the NOIR within a finite time period.
- 4) Every road element has at least one in-neighbor element or out-neighbor element, i.e., no road element is isolated in the NOIR ($\bigwedge_{i \in \mathcal{V}} \square (\mathcal{I}_i \cup \mathcal{O}_i \neq \emptyset)$).

V. TRAFFIC CONGESTION CONTROL

We use MPC to determine the boundary control $\mathbf{s}[k]$ at every discrete time k by solving a quadratic programming problem with quadratic costs and linear constraints imposing the feasibility conditions into management of traffic coordination. To this end, according to Eq. (15), we predict the traffic dynamics within the next N_τ sampling times by obtaining the following finite-horizon predictive model:

$$\mathbf{X}[k] = \mathbf{G}[k]\mathbf{x}[k] + \mathbf{H}[k]\mathbf{U}[k] \quad (17)$$

where

$$\mathbf{X}[k] = \begin{bmatrix} \mathbf{x}[k+1] \\ \vdots \\ \mathbf{x}[k+N_\tau] \end{bmatrix} \in \mathbb{R}^{(N-N_{out})N_\tau \times 1}, \quad (18a)$$

$$\mathbf{G}[k] = \begin{bmatrix} \mathbf{A}[k] \\ \vdots \\ \mathbf{A}^{N_\tau}[k] \end{bmatrix} \in \mathbb{R}^{(N-N_{out})N_\tau \times (N-N_{out})}, \quad (18b)$$

$$\mathbf{H}[k] = \begin{bmatrix} \mathbf{B}[k] & 0 & 0 & \cdots & 0 \\ \mathbf{A}[k]\mathbf{B}[k] & \mathbf{B}[k] & 0 & \cdots & 0 \\ \mathbf{A}^2[k]\mathbf{B}[k] & \mathbf{A}[k]\mathbf{B}[k] & \mathbf{B}[k] & \cdots & 0 \\ \vdots & \vdots & \vdots & \ddots & \vdots \\ \mathbf{A}^{N_\tau-1}[k]\mathbf{B}[k] & \mathbf{A}^{N_\tau-2}[k]\mathbf{B}[k] & \mathbf{A}^{N_\tau-3}[k]\mathbf{B}[k] & \cdots & \mathbf{B}[k] \end{bmatrix}, \quad (18c)$$

$$\mathbf{x}[k] = \begin{bmatrix} \rho_1[k] \\ \vdots \\ \rho_N[k] \end{bmatrix} \in \mathbb{R}^{(N-N_{out}) \times 1}, \quad (18d)$$

$$\mathbf{U}[k] = \begin{bmatrix} \mathbf{s}[k] \\ \vdots \\ \mathbf{s}[k+N_\tau-1] \end{bmatrix} \in \mathbb{R}^{(N_{out}N_\tau) \times 1}. \quad (18e)$$

The cost function C , previously defined in (8), can be rewritten as follows:

$$\begin{aligned} C(\mathbf{U}[k]) &= \frac{1}{2} \left(\mathbf{U}^\top[k]\mathbf{U}[k] + \beta \mathbf{X}^\top[k]\mathbf{X}[k] \right) \\ &= \frac{1}{2} \mathbf{U}^\top[k] \mathbf{W}_1[k] \mathbf{U}[k] + \mathbf{W}_2^\top[k] \mathbf{U}[k] + \mathbf{W}_3[k], \end{aligned} \quad (19)$$

where

$$\mathbf{W}_1[k] = \mathbf{I}_{N_{out}N_\tau} + \beta \mathbf{H}^\top[k]\mathbf{H}[k], \quad (20a)$$

$$\mathbf{W}_2^\top[k] = \beta \mathbf{x}^\top[k] \mathbf{G}^\top[k] \mathbf{H}[k], \quad (20b)$$

$$\mathbf{W}_3[k] = \frac{1}{2} \beta \mathbf{x}^\top[k] \mathbf{G}^\top[k] \mathbf{G}[k] \mathbf{x}[k]. \quad (20c)$$

Note that $\mathbf{W}_3[k]$ can be removed from cost function (19) since $\mathbf{W}_3[k]$ depends on $\mathbf{x}[k]$ at every discrete time k , but it is independent of $\mathbf{U}[k]$. Therefore,

$$C' = \frac{1}{2} \mathbf{U}^\top[k] \mathbf{W}_1[k] \mathbf{U}[k] + \mathbf{W}_2[k]^\top \mathbf{U}[k] \quad (21)$$

can be defined as the cost function of traffic coordination, and the optimal control variable

$$\mathbf{s}^*[k] = [\mathbf{I}_{N_{out}} \ \mathbf{0}_{N_{out} \times N_{out}(N_\tau-1)}] \quad (22)$$

is assigned by determining $\mathbf{U}^*[k]$ as the solution of the following optimization problem:

$$\min C' = \min \left(\frac{1}{2} \mathbf{U}^T[k] \mathbf{W}_1[k] \mathbf{U}[k] + \mathbf{W}_2^T[k] \mathbf{U}[k] \right)$$

subject to

$$\mathbf{W}_4[k] \mathbf{U}[k] + \mathbf{W}_5[k] \leq \mathbf{0}, \quad (23a)$$

$$\mathbf{W}_6[k] \mathbf{U}[k] + \mathbf{W}_7[k] = \mathbf{0}, \quad (23b)$$

where

$$\mathbf{W}_4[k] = \begin{bmatrix} -\mathbf{I}_{N_{out} N_\tau} \\ \mathbf{H}[k] \\ -\mathbf{H}[k] \end{bmatrix}, \quad (24a)$$

$$\mathbf{W}_5[k] = \begin{bmatrix} \mathbf{0}_{N_{out} N_\tau \times 1} \\ -\mathbf{1}_{(N-N_{out}) N_\tau \times 1} \otimes \mathbf{x}_{\max} + \mathbf{G}[k] \mathbf{x}[k] \\ -\mathbf{G}[k] \mathbf{x}[k] \end{bmatrix}, \quad (24b)$$

$$\mathbf{W}_6[k] = \mathbf{I}_{N_\tau} \otimes \mathbf{1}_{1 \times N_{out}}, \quad (24c)$$

$$\mathbf{W}_7[k] = -d_0 \mathbf{1}_{N_\tau \times 1}. \quad (24d)$$

Theorem 2. *The traffic density at every interior road element and discrete time k satisfies the inequality equation*

$$\rho_i[k] \geq 0, \quad \forall i \in \mathcal{V}_I \cup k \geq 1, \quad (25)$$

if conditions

$$\rho_i[1] \geq 0, \quad \forall i \in \mathcal{V}_I, \quad (26a)$$

$$u_j[k] \geq 0, \quad \forall j \in \mathcal{V}_{in}, \quad (26b)$$

$$v_n[k] \geq 0, \quad \forall n \in \mathcal{V}_{out}, \quad (26c)$$

hold.

Proof: See the proof in [15].

Remark 1. Per Theorem 2, it is ensured that the traffic density is non-negative at every discrete time k , if conditions (26) hold. Therefore, constraint Eq. (23a) simplifies to

$$\begin{bmatrix} -\mathbf{I}_{N_\tau N_{out}} \\ \mathbf{H}[k] \end{bmatrix} \mathbf{U}[k] + \begin{bmatrix} \mathbf{0}_{N_\tau N_{out} \times 1} \\ -\mathbf{1}_{(N-N_{out}) N_\tau \times 1} \otimes \mathbf{x}_{\max} + \mathbf{G}[k] \mathbf{x}[k] \end{bmatrix} \leq \mathbf{0}. \quad (27)$$

VI. SIMULATION RESULTS

In this section, we illustrate the simulation results of the traffic control based on a part of real street map of the Philadelphia Center City which is composed of 259 road elements (See Fig. 1). In order to denote and manage the road elements in the map conveniently, we assign specific indices for every road element in the NOIR. According to the road types, the road elements set $\mathcal{V} = \{1, \dots, 259\}$ is partitioned to $\mathcal{V}_{in} = \{1, \dots, 20\}$, $\mathcal{V}_{out} = \{21, \dots, 42\}$, and $\mathcal{V}_I = \{43, \dots, 259\}$.

We randomly assign the initial traffic density $\rho_i[0]$ at every road element $i \in \mathcal{V}$ in the NOIR and run the simulation for 300 time steps, where sampling time k represents the continuous time interval $[t_k, t_{k+1})$ and $\Delta t = t_{k+1} - t_k$ is constant at every discrete time k . At each sampling time k , the flow probability matrix $\mathbf{P}[k]$ and fraction probability matrix $\mathbf{Q}[k]$ are randomly generated.

For simulation, we ignore the inter-vehicle distance and assume that the length of vehicle l_{veh} is equal to 4.5m and obtain the maximum traffic density $\rho_{i,max}$ for every interior road element $i \in \mathcal{V}_I$ by

$$\rho_{i,max} = \frac{n_{i,lane} \times l_i}{l_{veh}}, \quad (28)$$

where l_i is the length of the road element i obtained from the street map data and $n_{i,lane}$ is the number of lanes in road element $i \in \mathcal{V}_I$. Furthermore, we assume that 400 cars can cross the boundary of the NOIR during the interval $[t_k, t_{k+1})$ at every sampling time k . Therefore, $d_0 = 400$ is used in equality constraint (24d).

The simulation is run under different scaling parameters $\beta = 0$, $\beta = 0.5$ and $\beta = 1$ that are used to weigh the cost function (19). The results are presented for two boundary inlet, boundary outlet, and interior road elements with index numbers and locations presented in Table I.

Road Type	Road Element Index	Name and Location
Inlet	9	Chestnut St. between S19th St. and S20th St.
Inlet	12	Sansom St. between S9th St. and S10th St.
Outlet	28	Filbert St. between S9th St. and S10th St.
Outlet	33	Arch St. between N19th St. and N20th St.
Interior	150	Market St. between N16th St. and N17th St.
Interior	239	Walnut St. between S15th St. and S16th St.

TABLE I: Example road elements in NOIR

We illustrate the variation of the optimal external traffic flow s_i at the example road elements under different values of β throughout the whole simulation time in Figs. 3 and Fig. 4. It is observed that the external traffic flow of the inlet road elements u_i and outlet road elements v_i hold similar properties at different values of β , that is: the external traffic inflow and outflow reach the steady state condition after about 20 sampling times. For $\beta = 0$, the weight matrix $\mathbf{W}_1[k]$ is diagonal at every discrete time k , but $\mathbf{W}_1[k]$ is not diagonal and $\mathbf{W}_2^T[k]$ also not equals to $\mathbf{0}$ when $\beta > 0$ is selected. Therefore, we observe that the variations of external flow are different when $\beta = 0$ is selected. In addition, it is observed that that the plots have large fluctuations when $\beta > 0$ due to the variation of the number of existing cars in the interior road elements.

Fig. 5, plots variations of $\rho_{150}[k]$ and $\rho_{239}[k]$ at different sampling times k ($k \in \{1, \dots, 300\}$). Although, variation curves of traffic densities at interior road elements have a large fluctuation, we could still observe an stable tendency after a certain period of time.

The number of vehicles entering and existing the NOIR during the whole simulation time are plotted in the Fig. 6 for $\beta = 0$. Consistent with the constraint Eq. (23b), the sum of vehicles crossing the border of the NOIR is equal to $d_0 = 400$ at every sampling time k . Starting from a larger value, the amount of external traffic inflow u_i gradually decreases

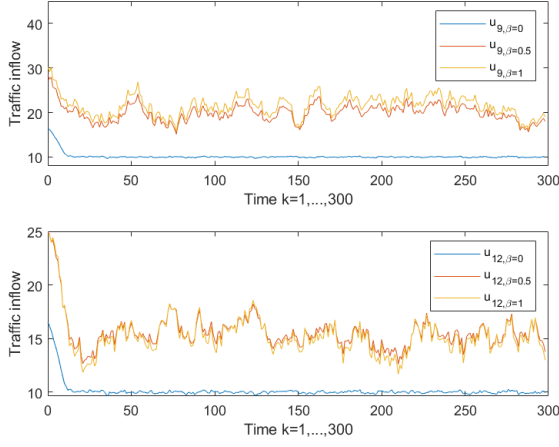


Fig. 3: External traffic inflows of inlet road elements under different β values

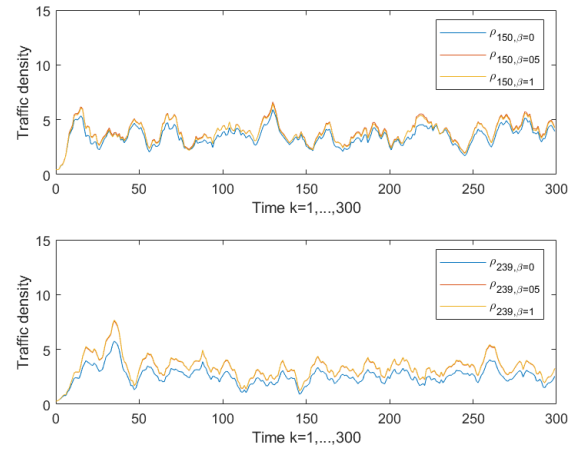


Fig. 5: Traffic densities of interior road elements under different β values

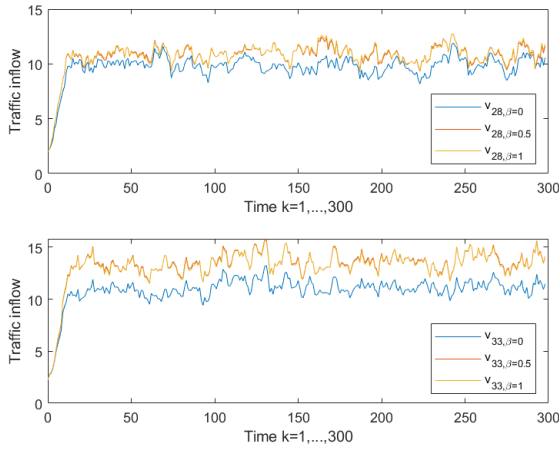


Fig. 4: External traffic outflows of outlet road elements under different β values

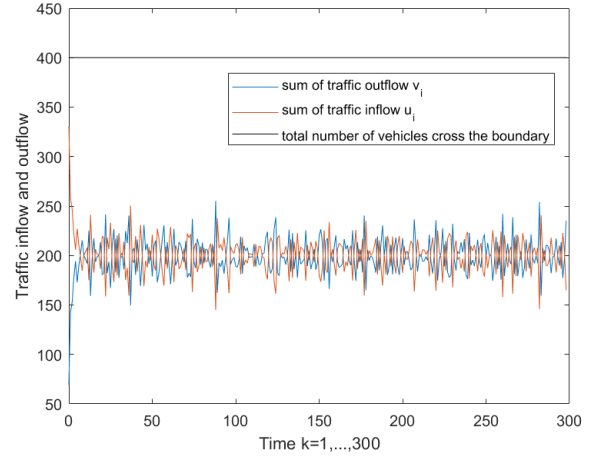


Fig. 6: External traffic inflow and outflow of the NOIR under $\beta = 0$

to a steady-state value at 200. It is seen that the external traffic outflow v_i symmetrically increases from a small value and reaches the steady state value at 200. The simulation results of external traffic flows for $\beta = 0.5$ and $\beta = 1$ shown in Fig. 7 illustrate a similar trend as when $\beta = 0$. Note the equilibrium (steady-state) condition, which implies that the traffic entering the NOIR is equal to the traffic existing from the NOIR, is first observed at $k \geq 20$ where

$$\forall k \geq 20, \sum_{i \in V_{in}} u_i[k] = \sum_{i \in V_{out}} v_i[k] \cong 200 \quad (29)$$

VII. CONCLUSION

This paper intruduces a physics-inspired approach based on the mass conservation law to model the traffic dynamics and implements the MPC method to control the boundary traffic inflow and outflow, so that the traffic congestion can be alleviated. Comparing with our previous research, the traffic dynamics model in this paper is more realistic. Simulation

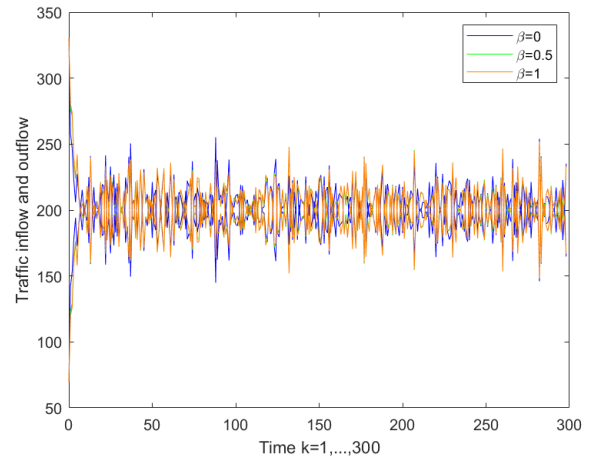


Fig. 7: External traffic inflow and outflow of the NOIR under different β values

applied in a area of Philadelphia Center City demonstrates that the proposed traffic model and control approach can achieve the objective of traffic congestion alleviation successfully through controlling the boundary traffic flow. Our further research will focus on the integration of the Makrov decision process (MDP) with the traffic dynamics model to control the traffic more efficiently and intelligently.

VIII. ACKNOWLEDGEMENT

This work has been supported by the Department of Mechanical Engineering at Villanova University. The authors would like to gratefully acknowledge Dr. Sergey Nersesov for the useful comments on this paper, and the Mechanical Engineering PhD fellowship provided to Xun Liu which was made possible by a generous gift from Dr. Yongping Gu and Fei Gu.

REFERENCES

- [1] H. Chin and M. Rahman, "An impact evaluation of traffic congestion on ecology," *Planning Studies and Practice*, vol. 3, pp. 32–44, 2011.
- [2] L. Ye, Y. Hui, and D. Yang, "Road traffic congestion measurement considering impacts on travelers," *Journal of Modern Transportation*, vol. 21, pp. 28–39, 2013.
- [3] J. Annan, J. Mensah, and N. Boso, "Traffic congestion impact on energy consumption and workforce productivity: empirical evidence from a developing country," *Archives of Business Research*, vol. 3, pp. 40–54, 2015.
- [4] C. P. Muneera and K. Karuppanagounder, "Economic impact of traffic congestion- estimation and challenges," *European Transport / Trasporti Europei*, vol. 68, 2018.
- [5] M. O'Mahony and H. Finlay, "Impact of traffic congestion on trade and strategies for mitigation," *Transportation Research Board*, vol. 1873, pp. 25–34, 2004.
- [6] N. Geroliminis and C. F. Daganzo, "Existence of urban-scale macroscopic fundamental diagrams: Some experimental findings," *Transportation Research Part B: Methodological*, vol. 42, no. 9, pp. 759 – 770, 2008. [Online]. Available: <http://www.sciencedirect.com/science/article/pii/S0191261508000180>
- [7] F. Xu, Z. He, Z. Sha, W. Sun, and L. Zhuang, "Traffic state evaluation based on macroscopic fundamental diagram of urban road network," *Procedia Social and Behavioral Sciences*, vol. 96, pp. 480–489, 2013.
- [8] I. I. Sirmatel and N. Geroliminis, "Integration of perimeter control and route guidance in large-scale urban networks via model predictive control," in *Transportation Research Board 96th Annual Meeting*. Transportation Research Board, 2017, p. 13p.
- [9] P. Shao, L. Wang, W. Qian, Q.-G. Wang, and X.-H. Yang, "A distributed traffic control strategy based on cell-transmission model," *IEEE Access*, vol. 6, pp. 10 771–10 778, 2018.
- [10] L. Munoz, X. Sun, R. Horowitz, and L. Alvarez-Icaza, "Traffic density estimation with the cell transmission model," vol. 5, 07 2003, pp. 3750 – 3755.
- [11] S. Yin, L. Yang, and K. Han, "Off-block flow optimisation based on cell transmission model," *DASC*, 04 2017.
- [12] O. Feldman and M. Maher, "A cell transmission model applied to the optimisation of traffic signals," 01 2002.
- [13] L. Yang, S. Yin, K. Han, J. Haddad, and M. Hu, "Fundamental diagrams of airport surface traffic: Models and applications," *Transportation Research Part B: Methodological*, vol. 106, pp. 29–51, 2017.
- [14] L. Yang, S. Yin, and M. Hu, "Network flow dynamics modeling and analysis of arrival traffic in terminal airspace," *IEEE Access*, vol. 7, pp. 73 993–74 016, 06 2019.
- [15] X. Liu and H. Rastgoftar, "Conservation-based modeling and boundary control of congestion with an application to traffic management in center city philadelphia," *arXiv preprint arXiv:2102.00552*, 2021.
- [16] H. Rastgoftar and E. Atkins, "An integrative data-driven physics-inspired approach to traffic congestion control," 2019.
- [17] Y. Zhang and R. Su, "An optimization model and traffic light control scheme for heterogeneous traffic systems," *Transportation Research Part C: Emerging Technologies*, vol. 124, p. 102911, 03 2021.

- [18] Q. Ba and K. Savla, "On distributed computation of optimal control of traffic flow over networks," in *54th Annual Allerton Conference on Communication, Control, and Computing*. IEEE, 2016, pp. 1102–1109.
- [19] H. Rastgoftar and J.-B. Jeannin, "A physics-based finite-state abstraction for traffic congestion control," 2021.
- [20] H. Rastgoftar and A. Girard, "Resilient physics-based traffic congestion control," 07 2020, pp. 4120–4125.
- [21] S. Lin, B. De Schutter, Y. Xi, and H. Hellendoorn, "Fast model predictive control for urban road networks via milp," *Intelligent Transportation Systems, IEEE Transactions on*, vol. 12, pp. 846 – 856, 10 2011.
- [22] Z. Li, S. Jin, C. Xu, and J. Li, "Model-free adaptive predictive control for an urban road traffic network via perimeter control," *IEEE Access*, vol. 7, pp. 172 489–172 495, 11 2019.
- [23] B. Abdulhai, R. Pringle, and G. Karakoulas, "Reinforcement learning for true adaptive traffic signal control," *Journal of Transportation Engineering*, vol. 129, 05 2003.
- [24] P. L.A. and S. Bhatnagar, "Reinforcement learning with function approximation for traffic signal control," *Intelligent Transportation Systems, IEEE Transactions on*, vol. 12, pp. 412 – 421, 07 2011.
- [25] Y. Lin, X. Dai, L. Li, and F.-Y. Wang, "An efficient deep reinforcement learning model for urban traffic control," 2018.
- [26] M. Gregurić, M. Vujić, C. Alexopoulos, and M. Miletić, "Application of deep reinforcement learning in traffic signal control: An overview and impact of open traffic data," *Applied Sciences*, vol. 10, p. 4011, 06 2020.
- [27] O. Adetoyi, "Development of sugeno fuzzy controlled traffic system for y-road intersection – university of ibadan case study," 11 2019.
- [28] M. Bhatia, A. Aggarwal, and N. Kumar, "Smart traffic light system to control traffic congestion pjaee, 17 (9) (2020) smart traffic light system to control traffic congestion," *PalArch's Journal of Archaeology of Egypt/ Egyptology*, vol. 17, pp. 7093–7109, 01 2021.
- [29] A. P. Zohar Manna, *The Temporal Logic of Reactive and Concurrent Systems*. Springer-Verlag New York, 1992.
- [30] T. Wongpiromsarn, U. Topcu, and R. Murray, "Receding horizon temporal logic planning for dynamical systems," 12 2009, pp. 5997–6004.
- [31] R. Koymans, "Specifying real-time properties with metric temporal logic," *Real-Time Systems*, vol. 2, p. 255–299, 1990.
- [32] Z. Qu, *Cooperative Control of Dynamical Systems*. Springer-Verlag London, 2009.

APPENDIX

Proof of Theorem 1: Given the above definitions, matrix $\mathbf{Q}[k]\mathbf{P}[k]$ holds the following properties:

- 1) All entries of matrix $\mathbf{Q}[k]\mathbf{P}[k]$ are non-negative.
- 2) Since no isolated interior road element exists in the NOIR, entries of column $i \in \{1, \dots, N - N_{out}\}$ of $\mathbf{Q}[k]\mathbf{P}[k]$ sum up to a positive value in the interval $(0, 1)$.

Given the above characteristics, the spectral radius of matrix $\mathbf{Q}[k]\mathbf{P}[k]$ is less than 1 at every sampling time k [32]. Then, according to the Neumann series theorem, we can rewrite the matrix $(\mathbf{I} - \mathbf{Q}[k]\mathbf{P}[k])^{-1}$ as follows:

$$(\mathbf{I} - \mathbf{Q}[k]\mathbf{P}[k])^{-1} = \sum_{h=0}^{\infty} (\mathbf{Q}[k]\mathbf{P}[k])^h. \quad (30)$$

Pre-multiplying both sides of (30) by $(\mathbf{I} - \mathbf{Q}[k]\mathbf{P}[k])$, we obtain

$$\begin{aligned} & (\mathbf{I} - \mathbf{Q}[k]\mathbf{P}[k]) (\mathbf{I} - \mathbf{Q}[k]\mathbf{P}[k])^{-1} \\ &= \sum_{h=0}^{\infty} (\mathbf{Q}[k]\mathbf{P}[k])^h - \sum_{h=0}^{\infty} (\mathbf{Q}[k]\mathbf{P}[k])^{h+1} \\ &= \lim_{h \rightarrow \infty} (\mathbf{I} - (\mathbf{Q}[k]\mathbf{P}[k])^{h+1}) = \mathbf{I}. \end{aligned} \quad (31)$$

Since every entry of matrix $\mathbf{Q}[k]$ is non-negative and sum of the elements of $N_{out} - N_{in}$ columns of matrix $\mathbf{Q}[k]$ are less than 1, the spectral radius of matrix $\mathbf{Q}[k]$ is less than 1 [32]. Then, the spectral radius of $\mathbf{Q}[k]\mathbf{P}[k]$ is less than the spectral radius of matrix $\mathbf{P}[k]$. Therefore, the spectral radius of matrix $\mathbf{I} - \mathbf{P}[k]$ is less than the spectral radius of matrix $\mathbf{I} - \mathbf{Q}[k]\mathbf{P}[k]$ which in turn implies that the spectral radius of matrix $\mathbf{A}[k] = (\mathbf{I} - \mathbf{P}[k])(\mathbf{I} - \mathbf{Q}[k]\mathbf{P}[k])^{-1}$ is less than 1 at every discrete time k .

Now, we can rewrite the traffic dynamics (15) as:

$$\mathbf{x}[k+1] = \Theta_k \begin{bmatrix} \mathbf{x}[1] \\ \mathbf{B}[1]\mathbf{s}[1] \\ \vdots \\ \mathbf{B}[k]\mathbf{s}[k] \end{bmatrix} \quad (32)$$

where

$$\Theta_k = [\Gamma_k \quad \cdots \quad \Gamma_1 \quad \Gamma_0] \quad (33a)$$

$$\Gamma_h = \prod_{j=k-h+1}^k \mathbf{A}[j] \quad (33b)$$

for $h = 1, \dots, k$, and $\Gamma_0 = \mathbf{I}_{N-N_{out}} \in \mathbb{R}^{(N-N_{out}) \times (N-N_{out})}$ is an identity matrix. Because the initial traffic density vector $\mathbf{x}[1]$ and control input vector $\mathbf{s}[k]$ are bounded, we can say:

$$\mathbf{x}[1] \leq z_{\max} \mathbf{1}_{N-N_{out} \times 1} \quad (34a)$$

$$\mathbf{B}\mathbf{s}[k] \leq z_{\max} \mathbf{1}_{N-N_{out} \times 1}, \quad (34b)$$

where z_{\max} is a sufficiently large value. Moreover, as shown in Eq. (33b), Γ_h is the product of matrices $\mathbf{A}[j]$. Therefore, we can draw the conclusion that the spectral radius of matrix Γ_h must also be less than 1 at every discrete time k , since the spectral radius of matrix $\mathbf{A}[k]$ is less than upper bound $r_a < 1$ at every sampling time k . Now, we calculate the norm of $\|\mathbf{x}[k+1]\|^2$ as follow:

$$\begin{aligned} \mathbf{x}^\top[k+1] \mathbf{x}[k+1] &\leq z_{\max} \mathbf{1}_{N-N_{out} \times 1}^\top \left(\sum_{l=0}^k \sum_{h=0}^k \Gamma_l^\top \Gamma_h \right) z_{\max} \mathbf{1}_{N-N_{out} \times 1} \\ &\leq z_{\max}^2 (N - N_{out}) \left(\sum_{l=0}^{\infty} r_a^l \right) \leq \frac{z_{\max}^2 (N - N_{out})}{(1 - r_a)}. \end{aligned} \quad (35)$$

which implies that $\|\mathbf{x}[k+1]\|^2$ is bounded at every discrete time k . Thus the BIBO stability of traffic dynamics (15) is proven.